Prediction of RCF clustered cracks dimensions using an ACFM sensor and influence of crack length and vertical angle

J. Shen[a,*], L. Zhou[a], H. Rowshandel[b], G.L. Nicholson[b], C.L. Davis[a,b]

a Advanced Manufacturing and Materials Centre, WMG, University of Warwick, Coventry, CV4 7AL, UK

b Birmingham Centre for Railway Research and Education, University of Birmingham, Birmingham B15 2TT, UK

*Corresponding author. E-mail address: Jialong.Shen@warwick.ac.uk; shenjialong2012@gmail.com

Abstract

Rolling contact fatigue (RCF) cracks are the predominant reason for rail grinding maintenance and replacement on all types of railway system, as they can potentially cause rail break if not removed. To avoid excessive material removal, accurate crack sizing is required. This is particularly the case for small cracks, which are typically in the form of crack clusters and appear with shallow propagation angles, and can be readily removed by grinding. Alternating current field measurement (ACFM) has been used as an electromagnetic method for RCF crack sizing, incorporating with modelling results for single RCF cracks with large vertical angles (> 30°). No study using this knowledge to size shallow angled crack clusters has yet been reported. A novel method, the pocket length compensation method, is proposed to determine the length and depth of RCF cracks with shallow vertical angles. It has been applied to machined crack clusters and to crack clusters in rails removed from service. For shallow (vertical angle < 30°) crack clusters, vertical angle predictions are close to the measured values with a deviation of less than 13.6 %. Errors in crack pocket length prediction are greatly reduced when the pocket length compensation was included. The predicted vertical depth using the approach developed for clustered angled cracks is accurate with errors < 8.3 %, which compares to errors of up to 60 % if the single RCF crack approach is used and errors of up to 21.4 % if a non-compensated prediction for crack clusters is used.

Keywords

Modelling, ACFM, RCF, clustered cracks, pocket length, vertical angle

Introduction

Rolling contact fatigue (RCF) cracks are a worldwide problem for rail maintenance and replacement on heavy-haul and passenger rail lines. RCF cracks initially propagate at a shallow vertical angle into the rail (typically 10°-30°), driven by the non-uniaxial traction of repeated loading between rails and wheels [3, 5-7]. The cracks can turn down after reaching a critical depth (typically 5 mm) potentially causing a rail failure, or turn up to the rail surface resulting in a spall [1-3]. RCF cracks usually present in the form of clusters consisting of varying size (surface length and pocket length, see Figure 1(a) and (c)), spacing, angle to the running direction (horizontal angle) and angle into the rail (vertical angle), due to variations in train speed, axle loads and rail grades [3, 4]. Regularly-sized RCF crack clusters are more common for rails mainly subjected to one type of traffic; variations in crack cluster patterns can reflect that the rail experienced a different mix of traffic [3]. For the example cracks shown in Figure 1a, the crack cluster has an average surface length of 18.5 mm and average crack spacing of 5.5 mm. Figure 1b shows more closely spaced cracks with cracks at the left being much shorter than the cracks at the right; the surface length ranges from 2.3 to 21.7 mm and the crack spacing ranges from 0.8 to 3.8 mm. Figure 1c shows a vertical cross section (along the running direction) through a crack cluster, also indicating the various pocket lengths and vertical angles into the rail. In this case pocket length ranges from 3.7 to 10.6 mm and vertical angle ranges from 16.4° to 38°.

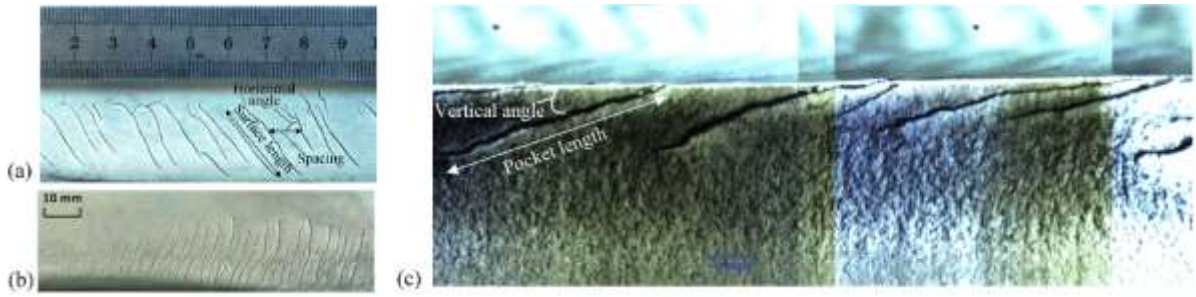

Figure 1 (a) Magnetic particle inspection (MPI) image showing RCF crack clusters on a rail sample taken from service; (b) MPI image of RCF cracks showing non-uniformly distributed cracks along the rail running direction; (c) a cross section of a crack cluster showing the cracks propagating into the rail.

The variation in crack size and cluster patterns presents a challenge to rail infrastructure managers in terms of inspection and maintenance, due to signal interactions between adjacent cracks causing difficulty in accurate characterisation, e.g. shadowing effect in ultrasonic inspection and characterisation approaches or calibration model being insufficient. Alternating current field measurement (ACFM) is an electromagnetic non-destructive technique being widely used in the underwater infrastructure, petroleum and rail industries

for crack detecting and sizing [8-11]. Recent research [15] showed promise to solve this challenge with contribution to characterisation of crack clusters and of shallow angled (30°) cracks, which until recently it was limited to showing the pocket length of individual cracks.

The ACFM exciting coil can induce a uniform current in the surface layer of the conductive material with no crack present. Any existence of a crack will disturb the current and force it to flow around the ends and down the faces of the crack; this causes the magnetic field generated by the induction current above the surface to become non-uniform and the ACFM sensor measures these variations in the field. The ACFM Bx signal as shown in Figure 2, can be used to effectively estimate the pocket length for single RCF cracks with a surface length less than 20 mm (i.e., the 'light' to 'moderate' cracks classified by Network Rail, UK [12]). The Bz signal is used to estimate the surface length for single RCF cracks, as the trough and the peak indicate the positions of the crack ends provided that the current flows perpendicular to the crack surface-breaking component. A raster scan is recommended for the most accurate crack surface length sizing. It can give crack surface angle information using Bx signal and this information then can be used to correct the probe angle before a final sizing scan is performed along the crack [13]. For crack clusters, The ACFM signal is normally measured across centres of cracks can reflect the distribution of Bx and Bz magnetic field. Any changes in crack parameters (surface length, vertical angle, inner spacing and crack number, etc.) can cause variation in magnetic field distribution and theses can also be detected through ACFM signals.

From a rail maintenance point of view, it is more important to know the crack vertical depth than the pocket length because this determines the amount of rail to be ground off to eliminate the RCF cracks before they grow to a severe size. Vertical depth varies depending on the crack vertical angle and crack pocket length, as shown in Figure 1c. It has recently been reported that the Bz trough-peak ratio, derived from a single measurement line across the centre of the crack at 45°, can be used to obtain the crack vertical angle, which can then be used with the determined crack pocket length to give the vertical depth [14]. This provides a guide for railway grinding to remove the RCF cracks.

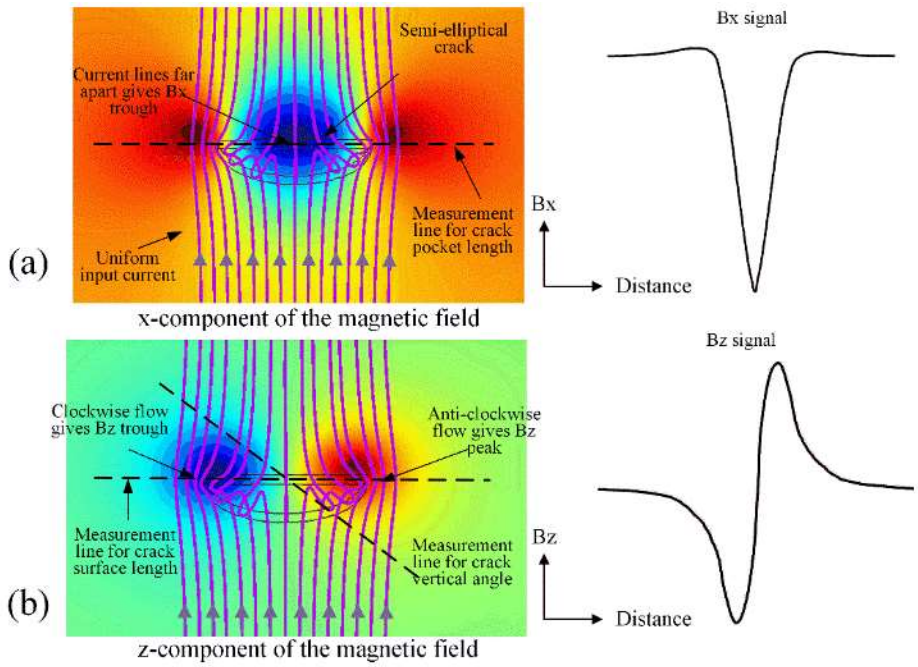

Figure 2 (a) The Bx magnetic field distribution and (b) the Bz magnetic field distribution around a single RCF crack showing the path (the dashed line) from which the Bx and Bz signals are extracted for crack pocket length, surface length and vertical angle determination [14].

The algorithm used for RCF crack dimension characterisation with an ACFM walking stick applied in rail inspection is based on theoretical results with empirical corrections for single cracks and crack shapes from experimental measurements on sectioned rails [15]. As crack spacing can vary, unless a large number of rails with varying crack configurations are sectioned any empirical corrections will only provide limited accuracy. RCF clusters with cracks that are closely spaced lead to an interaction between ACFM signals from each crack. Sizing for crack clusters using an algorithm based on modelling and measurements for single cracks inevitably leads to errors, as shown in [4]. Responses of ACFM Bx signals to various surface lengths, inner spacings and crack numbers for crack clusters have been reported but only cracks with vertical angles of > 30° were considered [16]. Previous studies [14, 22] have shown that shallow vertical angles (< 30°) give different Bx signals compared to those obtained for cracks with vertical angles >30° for single and clustered cracks, leading to under estimation of crack pocket lengths. It is important to be able to characterise crack clusters, as RCF cracks usually present in the form of clusters and with vertical angles less than 30°. Methods for sizing clusters of shallow (< 30°) RCF cracks have not been reported.

The modelling work initially focussed on signals from single isolated RCF cracks and size prediction and has progressed to predicting angle of propagation into the rail and considering

a uniform array of multiple cracks. In this paper the modelling capability has progressed significantly allowing for multiple cracks of varying geometry and configuration (e.g. size, spacing) to be considered. Modelling of crack clusters for shallow-angled cracks and the effect of vertical angles < 30° on the pocket length prediction is presented. A compensation method for pocket length determination in terms of different crack surface length, inner spacing and crack number is proposed. In addition the combined influence of crack propagation angle into the rail and multiple cracks has been considered for the first time. RCF crack clusters in rails removed from service, for the first time are used to verify the proposed compensation scheme and assess the improved prediction capability, respectively.

Model setup

A 3D finite element (FE) model was developed using the AC/DC module in COMSOL Multiphysics [17]. This model has been verified previously by experimental measurements for single cracks and uniformly sized crack clusters [4, 14, 16]. For the modelling work, RCF cracks are assumed to have a semi ellipse shape with elliptical ratios from 1 to 1.75, which has been shown to approximate real (light to moderate) RCF cracks in rails removed from service [3]. The model consists of a block representing a section of rail with the crack cluster at the surface and an air block above the rail section. The rail material considered in the model is a 260 grade rail steel. The electrical conductivity is set as 5×10^6 S/m and relative permeability as 50. The conductivity of air is assumed to be 50 S/m, as this aids the convergence of the model. This is particularly useful when modelling electromagnetic problems in Comsol. The maximum element size for the refined mesh block under the rail surface is 0.5 mm and the total number of meshing elements is in the order of 1.5×10^6. The model geometry and the standard Cartesian coordinates are shown in Figure 3a. Full details of the model and boundary conditions can be found elsewhere [14, 18, 19].

When sizing a RCF crack cluster using the ACFM pencil sensor, the sensor is usually oriented parallel to the crack and is moved to cross the centres of each crack with a path parallel to the running direction, as shown in Figure 3b. This ensures the current flows perpendicular to the cracks, in which case the field is maximally perturbed [18, 19]. In the present model, a uniform surface current is applied in a direction perpendicular to the crack surface-breaking component. The measurement line is set to be across the centres of each crack. This mimics a single scan using the physical ACFM pencil sensor over a crack cluster

with the sensor positioned with a horizontal angle of 45° to the rail running direction. Table 1 gives the summary of different parameter groups and values modelled in the paper.

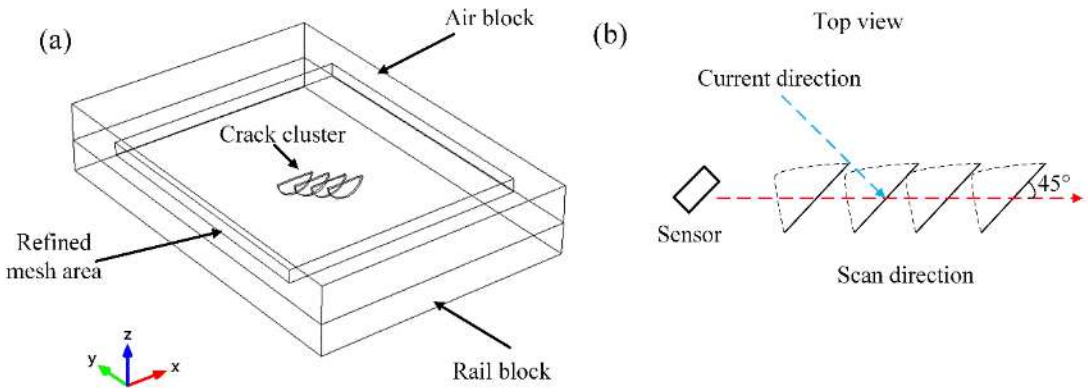

Figure 3 (a) Geometry of the model showing the refined mesh area for the crack cluster; (b) schematic diagram of the crack cluster arrangement and measurement line in the model, which mimics the physical ACFM measurements.

Table 1 Summary of the modelled parameters.

Parameters	Values
Surface length, mm	3, 9, 15, 21, 27, 33, 39
Inner spacing, mm	2, 4, 6, 8, 12, 16, 20
Crack number	3, 4, 5, 6, 9, 12, 15
Vertical angle, °	10, 20, 30, 90
Ratio (surface length/2×pocket length)	1, 1.25, 1.5, 1.75

Methodology

Shallow vertical crack angles, of 10, 20 and 30°, were selected for the modelling work in this paper. As there is no effect of vertical angle on the signals for cracks with vertical angles between 30 and 90° [14], 90° cracks were selected to be compared with the shallow angle results. For cracks with vertical angles less than about 30° there is an effect on ΔBx_{max} signal, with the shallower crack angles showing a larger effect [14]. The shallow vertical angle of 10° was selected to determine how large the sizing error is if vertical angle is not considered. The compensation values for pocket length determination considering shallow vertical angles can be applied to the results assuming the crack vertical angle is 90^{o} or there is no vertical angle effect on Bx signals.

Crack clusters 1 and 2 (shown in Figure 4) were scanned by the ACFM probe sensor before destructive inspection (progressive milling) was carried out to investigate their sub-surface dimensions (vertical angle and pocket length). From the ACFM grid scanning, the Bz trough-peak ratio (Bz_{trough}/Bz_{peak}) can be obtained and can be used to predict the vertical angle, where Bz_{trough} and Bz_{peak} are the minimum and the maximum recorded values of the z-component of the magnetic field, respectively along the measurement line [14]. The normalised change in Bx signal is used for the pocket length determination in this paper, i.e. normalised $\Delta Bx_{max} = (Bx_0 - Bx_{max})/Bx_0$ %. It indicates the decrease in the magnetic field over the crack, where Bx_0 is the background signal taken from an area free of cracks. ΔBx_{max} can also be used to compare the numerically and experimentally determined signals. The predicted pocket length and hence the vertical depth of clustered cracks can then be compared with the actual dimensions and the influence of vertical angle on crack dimension prediction can be discussed. The destructive milling started at 9 mm away from the gauge side and a total of 29 mm was milled off (each milling cycle removed 1 mm) to investigate the actual crack profiles of the RCF cracks.

Modelling for pocket length compensation

In this section the influences of shallow vertical angles on Bx signals in terms of variations of surface length, inner spacing and crack number for clustered cracks will be modelled and discussed. The compensation values for crack pocket length determined by the vertical angle can be obtained and can be used to improve the accuracy of the dimension prediction, which will be shown in the next section.

Variation of surface length

The cracks modelled are planar and semi elliptical in shape (elliptical ratio from 1 to 1.75) with surface lengths from 3 to 40 mm in order to cover the whole range of RCF cracks included in the GB railway classification system [12], although in practice larger cracks may have more complex shapes and be non-planar (turning down into the rail). Figure 4 shows the distribution of magnetic flux density and current streamlines around a crack cluster (surface length 15 mm, inner spacing 4 mm and crack number 4) with vertical angles of 90 and 10°. The area (dark blue) of low magnetic flux density (i.e. higher $\Delta Bx_{max}/Bx_0$ value) in the contour plot is caused by the sparse current streamlines when current flows down the crack surface. The side view in Figure 4b shows that for cracks with a vertical angle of 10° the

current flows along the crack surface and when it flows back to the sample surface, it takes a shorter pathway rather than being completely bound to the crack surface, which is the case for cracks with a vertical angle of 90°. This causes the greatest current intensity (dark blue area) behind the crack to move further from the crack opening and the measurement line. Signals extracted from the measurement line therefore show smaller values for the vertical angle of 10° than 90°. Further magnetic flux distribution figures (for changing vertical angle) can be found elsewhere [14].

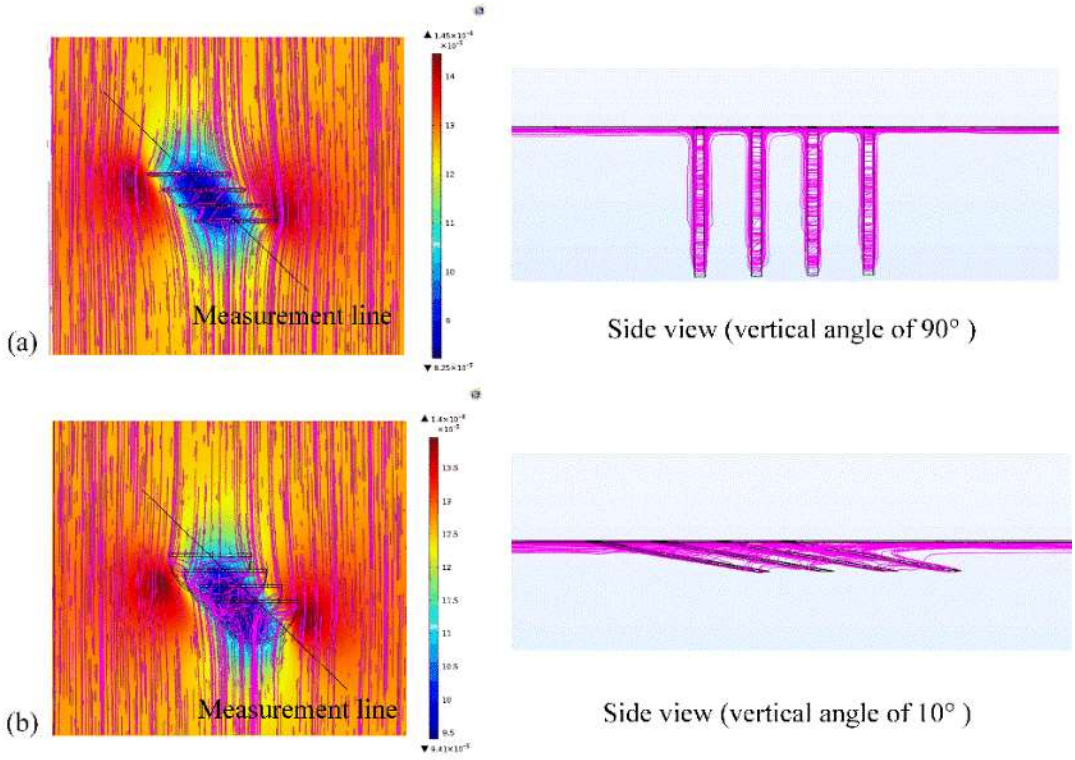

Figure 4 Distribution of magnetic flux density and current streamlines around crack clusters with vertical angle of (a) 90° and (b) 10° (crack surface length of 15 mm with inner spacing of 4 mm and crack number of 4).

Figure 5 shows the modelled signal results for cluster (4 mm inner spacing and crack number of 4) when the vertical angle is 90° and 10° together with the results for single RCF cracks (with vertical angle of 90°) taken from [19]. The normalised maximum ΔBx value for the cluster increases steeply as the surface length increases from 3 mm but begins to saturate when the surface length is above around 27 mm. This means for the uniformly sized cracks in the clusters presented in this study, the ACFM Bx signal can be effectively differentiated for cracks from the light to the heavy category [12] assuming an elliptical shape. It can be seen

from Figure 5a that the signal for clustered cracks is significantly larger than for single cracks so using a calibration curve developed for single cracks would give considerable errors in sizing. As shown in Figure 5b, cracks with a vertical angle of 10° decrease the maximum ΔBx compared to cracks with a vertical angle of 90°, with an average difference of 30.1 % (this is the difference in $\Delta Bx_{max}/Bx_0$ (given as a percentage) between the signal for a 90° vertical angle crack and for a 10° vertical angle crack, which gives a general idea about the difference effects of vertical angles) for all elliptical ratios and surface lengths. This is due to the reduced current density and the shift in the minimum value of the Bx magnetic field for shallower angles, as discussed in [14] for single cracks.

For accurate sizing of pocket lengths, the maximum ΔBx should be adjusted for, to take into account vertical angle. Figure 6 shows ratios between ΔBx_{max} from the vertical angle of 90° and shallow angles (30° and 10°) against crack surface length ($\Delta Bx_{max\_90°}/\Delta Bx_{max\_shallow\ angle}$). Cracks with surface lengths less than 3 mm are not considered as they are outside the range that ACFM is normally used for and do not give reliable signals. For cracks with shallow vertical angle of 30° the ratio is relative small while it begins to increase for angle of 10° with surface length less than 21 mm. This indicates the compensation of ΔBx_{max} for shallow vertical angle (< 30°) with 'light' to 'moderate' surface length is needed if sizing base on a value obtained from cracks with large vertical angles.

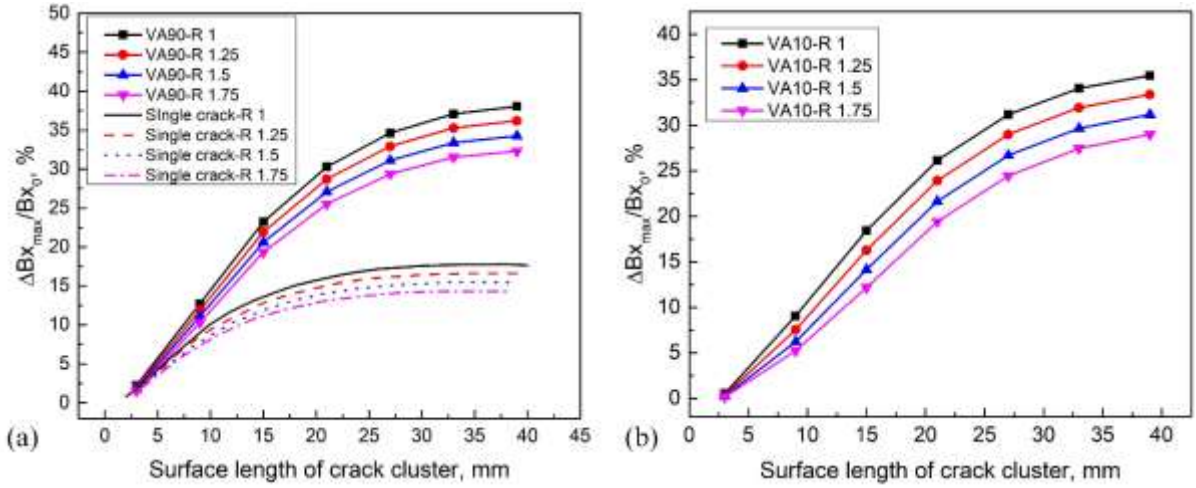

Figure 5. Modelling results for Bx signal response to variations of surface length when the crack vertical angle is (a) 90° and (b) 10°; the calibration curves for single cracks with semi ellipse shape from the literature [19] are also shown in (a); VA denotes the vertical angle and R denotes the elliptical ratio (uniformly sized cracks within the clusters with inner spacing of 4 mm and crack number of 4).

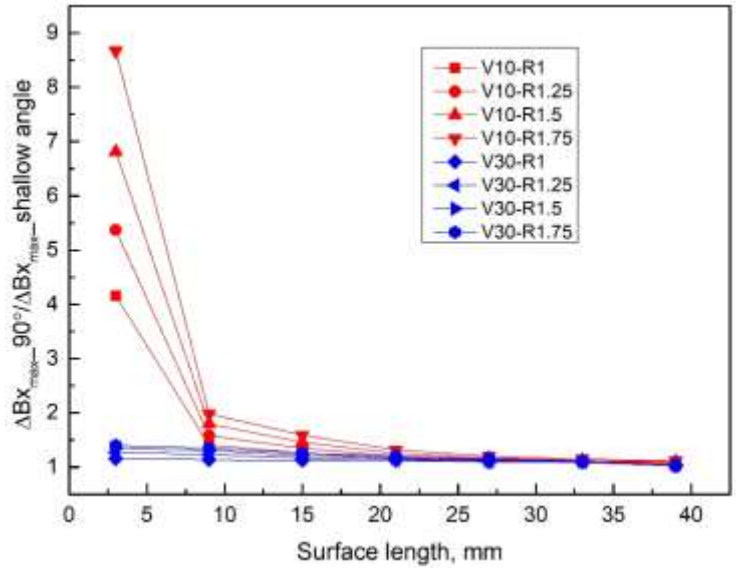

Figure 6. Ratio between ΔBx_{max} from the vertical angle of 90° and shallow angles against crack surface length.

Variation of inner spacing

The inner spacing (distance between adjacent cracks in a cluster) of RCF crack clusters has been reported to vary from 0.8 mm to 20 mm [2] for different rail grades, rail radius of curvature and traffic types. A large number of simulations were carried out to investigate the effect of crack inner spacing on the Bx signal responses and were used in a neural network [16]. Larger inner spacing will increas the interval of areas of low magnetic flux density caused by each crack in the cluster. This decreases the overlapping of the low magnetic flux areas and signal will decrease as inner spacing increases. It was found in [16] that with a fixed vertical angle of 30°, the effect of inner spacing on the signal is mostly dependent on the crack surface length (for a fixed elliptical ratio); this dependency intensifies with increasing surface length and weakens with decreasing surface length becoming insignificant for surface length < 5 mm. It was also found that the Bx signals saturate at inner spacing > 10 mm in the case of surface length < 20 mm (i.e. increasing spacing has no further effect on the signal) while there is still a weak influence for surface length > 20 mm. The influence of changing vertical angle to include shallow angles (< 30º) on the Bx responses to clustered cracks was not considered - since it has been shown to affect the Bx signal then this is now required to determine the level of compensation needed when sizing the pocket length for shallow angled clustered RCF cracks.

Uniformly sized crack clusters containing 4 cracks with crack inner spacings from 2 to 20 mm have been investigated. In Figure 7 it can be seen that the $\Delta Bx_{max}/Bx_0$ value decreases as

the crack inner spacing increases with inner spacing no longer having any significant influence above a spacing of about 12 mm for both vertical angle cases for the crack surface length of 12 mm. This is slightly higher than the value (10 mm) found in [16] which may be due to a different number of cracks being used in the study for the influence of inner spacing and / or how the effect has been determined. In addition the shallower vertical crack angle (10°) decreases the $\Delta Bx_{max}/Bx_0$ value when compared with the results for vertical angle of 90°. It has been found that when the ratio of surface length to inner spacing is smaller than a value of 1, the Bx signals correspond to those expected for a single crack, i.e. there is no influence of the neighbouring cracks. Therefore the surface length to inner spacing ratio can be used to indicate when crack sizing can be carried out using the calibration curve for single cracks or the influence of crack clusters needs to be taken into account. Table 2 lists the Bx compensation to account for shallow vertical angles of 30, 20 and 10° for the change of inner spacing in the clustered crack cases presented (elliptical ratio of 1). The compensation values decrease as inner spacing increases and reach a fixed value when the inner spacing is about 12 mm. The difference in $\Delta Bx_{max}/Bx_0$ between shallow vertical angles (10-30°) and 90° should be considered when using the ACFM signal to characterise the pocket length of the crack cluster.

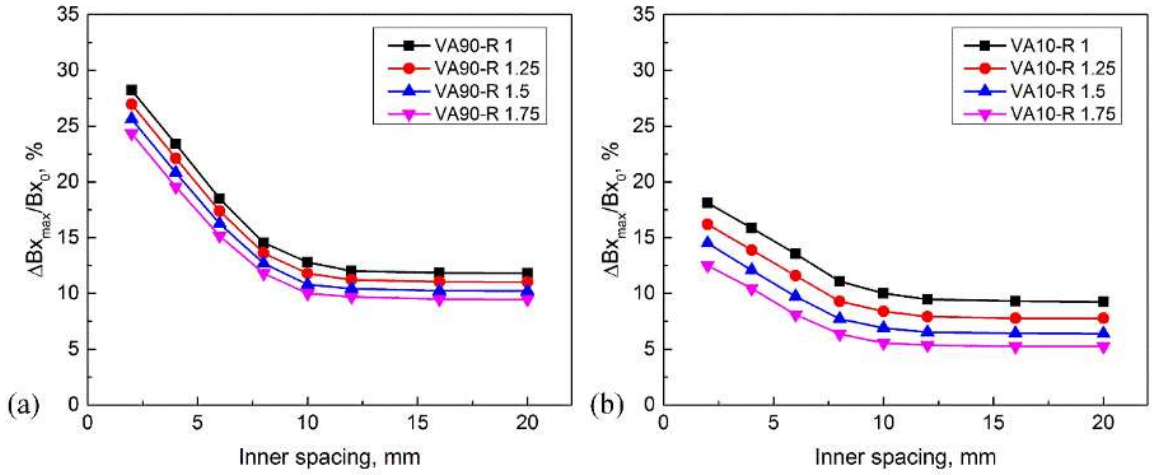

Figure 7. Modelling of Bx signals corresponding to variations of inner spacing for clusters of 4 uniformly sized cracks with surface length of 12 mm when the crack vertical angle is (a) 90° and (b) 10°; VA denotes the vertical angle and R denotes the elliptical ratio.

Table 2 Summary of the pocket length compensation ($\Delta Bx_{max}/Bx_0$) for shallow vertical angles in terms of the change of crack inner spacing (elliptical ratio of 1, surface length 12 mm, crack number 4).

Inner spacing, mm	2	4	6	8	12	16	20

ΔBx_{max} (vertical angle 90°) %	28.2	23.4	18.5	14.5	12.1	11.8	11.8
ΔBx_{max} compensation (vertical angle 30°) %	3.1	2.2	1.5	1.1	0.7	0.7	0.7
ΔBx_{max} compensation (vertical angle 20°) %	5.6	4.1	3.0	2.1	1.3	1.2	1.2
ΔBx_{max} compensation (vertical angle 10°) %	10.1	7.8	5.0	3.4	2.6	2.5	2.5

Variation of crack number

In practice, the number of cracks present in a cluster is variable and hence influence the Bx signal for crack pocket length prediction [4]. A previous study [4] showed the effect of crack number for crack clusters (surface length of 10 mm) with an inner spacing of 1 mm; it was shown that for crack clusters comprised of cracks with a vertical angle of 25°, the normalised Bx signals decreased as the crack number increased with the signal saturating at a crack number of >12. This is because increase of crack number will increase the overlapping area of low magnetic flux and this will increase the signal extracted from the low magnetic flux area. The ACFM neural network [16] developed for crack cluster pocket length prediction was based on a large number of simulations focusing on up to 17 within a cluster with a crack inner spacing from 1 to 12 mm (cracks with a vertical angle of 30°); it was shown that for surface length $\leqslant$ 5 mm the influence of crack number on the Bx signals is insignificant, whereas for surface length > 5 mm the effect of crack number on the signal depends only on the value of inner spacing and this dependency weakens with increasing inner spacing. In that work the role of vertical angle was not considered and is discussed here.

Figure 8 shows the influence of crack number on the Bx signals when the vertical angle is 90° and 10°. The $\Delta Bx_{max}/Bx$ value with vertical angle of 90° increases when the crack number increases up to 9 then the value saturates for all elliptical ratios studied. The $\Delta Bx_{max}/Bx$ value for the cluster with the shallow vertical angle (10°) is significantly lower than that for the 90° vertical angle, as seen previously. Table 3 lists the ΔBx_{max} compensation values for vertical angles of 30, 20 and 10°, against the change of crack number in the crack cluster with elliptical ratio of 1. The compensation values for all shallow vertical angles increase as the crack number increases but saturate at certain values as shown in Table 3. The compensation difference caused by crack number however is not that notable as the case when surface length or inner spacing vary, as changing of crack number does not alter the crack size (surface and pocket length) and crack arrangement (inner spacing).

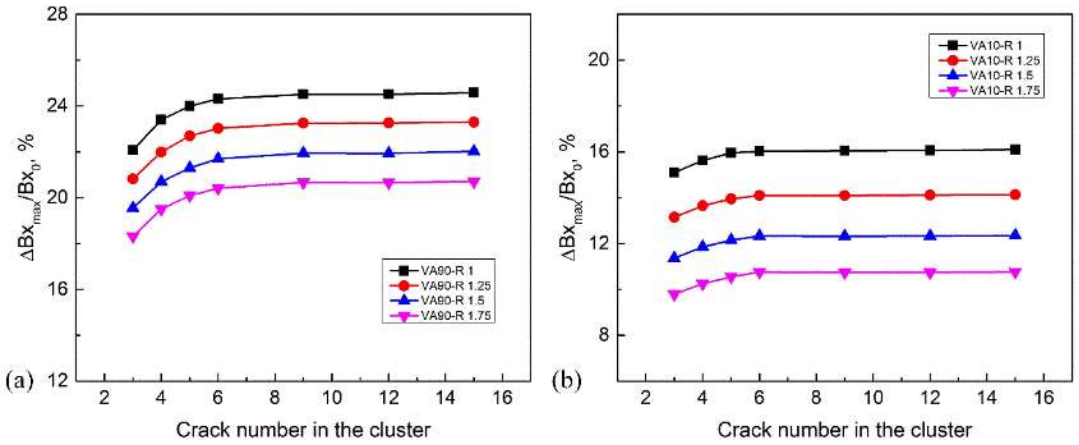

Figure 8. Modelling of Bx signal response to the variations of crack number for uniformly sized crack clusters with surface length of 12 mm and inner spacing of 4 mm when the vertical angle is (a) 90° and (b) 10°; VA denotes the vertical angle and R denotes the elliptical ratio.

Table 3 Summary of the pocket length compensation ($\Delta Bx_{max}/Bx_0$) for shallow vertical angles in terms of the change of crack number (elliptical ratio of 1, surface length 12 mm, inner spacing 4 mm).

Crack number	3	4	5	6	9	12	15
ΔBx_{max} (vertical angle 90°) %	22.1	23.4	24.0	24.3	24.5	24.5	24.5
ΔBx_{max} compensation (vertical angle 30°) %	20.6	21.8	22.5	22.8	22.8	22.8	22.8
ΔBx_{max} compensation (vertical angle 20°) %	18.6	19.5	19.9	20.3	20.3	20.3	20.3
ΔBx_{max} compensation (vertical angle 10°) %	15.1	15.5	15.8	16.1	16.1	16.1	16.1

It is expected that the influence of crack number on ΔBx_{max} depends on the crack surface length and inner spacing of the cluster. It can indicate that for crack cluster that have large inner spacing the crack number may not effect on Bx signals as less effects are seen for adjacent cracks. Figure 9 shows the $\Delta Bx_{max}/Bx_0$ value for crack clusters (vertical angle of 90° and 10°) with 15 mm surface length but with different inner spacings (3-6 mm), which gives surface length to spacing ratios from 5 to 2.5. For clusters with vertical angle of 90°, the $\Delta Bx_{max}/Bx_0$ value saturates at a larger value of crack number when the ratio of the crack surface length to the crack inner spacing increases, e.g. in Figure 8a, the $\Delta Bx_{max}/Bx_0$ value saturates at a crack number of 9 for the cluster with surface length of 15 mm and inner spacing of 3 mm (surface length to spacing ratio of 5) while the $\Delta Bx_{max}/Bx_0$ value saturates at a crack number of 6 for the cluster with surface length of 15 mm and inner spacing of 6 mm (surface length to spacing ratio of 2.5). The $\Delta Bx_{max}/Bx_0$ value for vertical angle of 10° however saturates at smaller crack number than the 90° case, i.e. as shown in Figure 9b, the

value saturates at crack number of 8 for surface length to spacing ratio of 5 and there is virtually no influence of crack number for surface length to spacing ratio of 2.5. Therefore shallow vertical angles reduce the influence of crack number change on the ΔBx_{max} values and the influence also decreases with a smaller surface length to inner spacing ratio. Therefore vertical angle should also be considered when studying the influence of crack number, rather than the parameter of inner spacing alone, as stated in [14], however for clusters (surface length to spacing ratio of 2.5) with vertical angles of 10° there is no need to consider the influence of crack number on Bx signals.

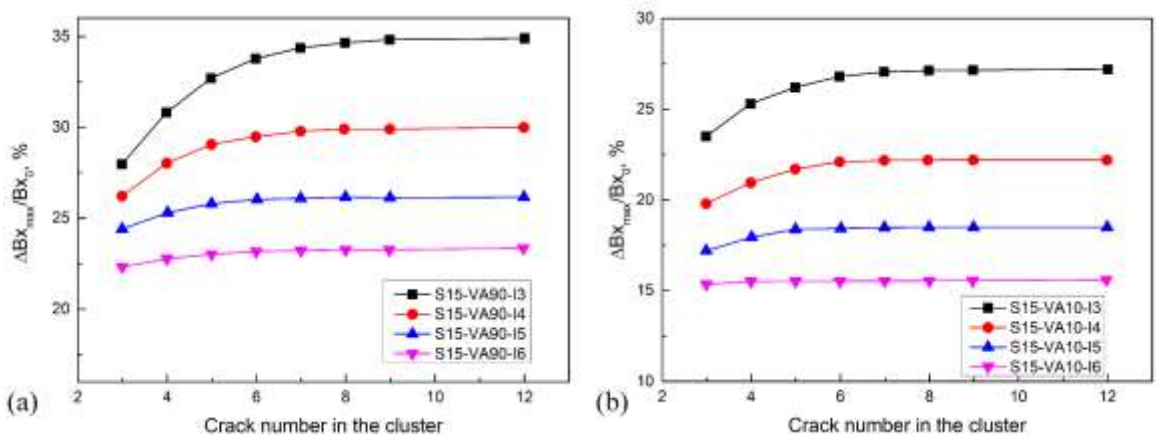

Figure 9 Modelling of Bx signals response to the variations of crack number for uniformly sized crack cluster with surface length of 15 mm and inner spacing of 3-6 mm (i.e. surface length to spacing ratio of 5 to 2.5) when vertical angle is (a) 90° and (b) 10°; S denotes the surface length, VA denotes the vertical angle and I denotes the inner spacing.

Case study on cracks taken from service

In this section ACFM grid measurement has been carried out on two crack clusters of the rail sample taken from the service. The pocket length and vertical depth for crack clusters will be predicted from Bx and Bz signals. The pocket length compensation will be considered according to the measured vertical angle and the vertical depth after the compensation will be compared and discussed.

Experimental measurement

Two RCF crack clusters (clusters 1 and 2) on a rail sample taken from service (high rail from BNSF, Canada; manufacture year of 1972), as shown in Figure 10a, were selected to be grid scanned by using the ACFM pencil sensor installed on a robotic arm (LR-Mate 200iD, FANUC UK Limited). The robotic arm allowed accurate control of lift off distance (0 mm in

the present study) between the single pencil probe and the railhead through the use of a laser range sensor (a commercial ACFM walking stick or array probe configuration would give constant lift off). The robotic arm was used to carry out 21 parallel scans (each scan 1 mm apart) forming the grid scanning area. The ACFM pencil sensor was held at 0 mm lift-off to the rail surface at 45° to the running direction (which is similar to the average horizontal angle of the inspected cracks).

Figure 10a shows the multiple cracks after MPI inspection (samples were first painted white and then the magnetic particle ink was sprayed to the sample surface; a magnetic yoke was used to magnetize the sample and magnetic particles accumulate on the crack surface breaking component revealing the crack appearance). Table 4 gives the dimensions of crack clusters 1 and 2. The cracks can be considered as two separate clusters because the spacing between these two clusters is larger than 13 mm (the discontinuous crack, underlined in blue, has been excluded as it was found, from the cross section, that it was very short and would not influence the ACFM signals significantly) and the crack spacing needed to avoid the influence of adjacent cracks on the signal from the ACFM pencil probe for these two clusters was determined to be 12.7 mm (surface length/inner spacing > 1; as discussed later). After ACFM scanning the rail was destructively examined using progressive milling to remove approximately 1 mm layers from the gauge corner through the RCF cracks. MPI inspection was used after each layer removal to allow the 3D character of the cracks to be revealed.

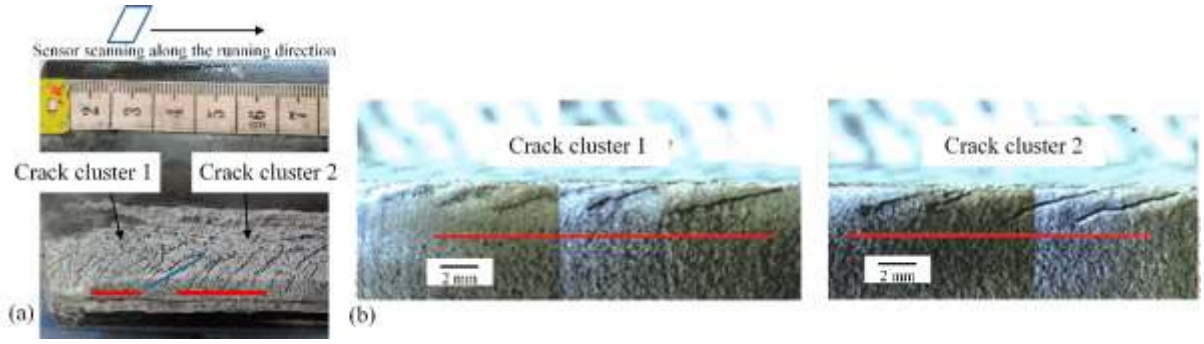

Figure 10 (a) The crack cluster inspected through ACFM grid scanning; (b) sectioned rail (sectioned along the running direction approximately at the mid-crack surface length position) showing the sub-surface crack length.

Table 4 Summary of the crack dimensions measured for clusters 1 and 2 shown in Figure 10 (average values are shown with the range of values shown in bracket).

Crack clusters	1	2
Surface length, mm	11.6 (10.5-14.3)	12.7 (10.8-15.6)

Pocket length, mm	5.4 (3.0-7.3)	7.3 (4.4-9.0)
Horizontal angle, °	43.3 (29.7-52.8)	43 (41.6-46.7)
Vertical angle, °	28.6 (25.8-30.7)	24.2 (20.9-24.8)
Inner spacing, mm	3.9 (2.7-4.8)	4.4 (1.9-6.1)
Crack number	4	4

Model validation

RCF crack clusters 1 and 2 (shown in Figure 10) on the sample taken from service were selected as the validation case study for sizing clustered cracks pocket length compensation (obtained from the previous section). Figure 11 shows a map of the x and z components of the magnetic field reconstructed from the ACFM grid scanning signals. Cracks are assumed to be straight and are represented as black lines in the figure indicating the crack arrangements. The Bz signals in Figure 11b indicate that the cracks form two clusters from the two distinct red areas indicating high Bz values, the distinction is less clear in the Bx signals. The crack spacing (discussed above) was used to classify the cracks into the two clusters. From the magnetic field mapping, the minimum value of the Bx magnetic field (for pocket length) and the minimum and maximum values of the Bz magnetic field (for vertical angle) can be accurately determined. This scenario represents scanning with an array probe [15] or a single probe using a robotic system carrying out multiple scans [20, 21].

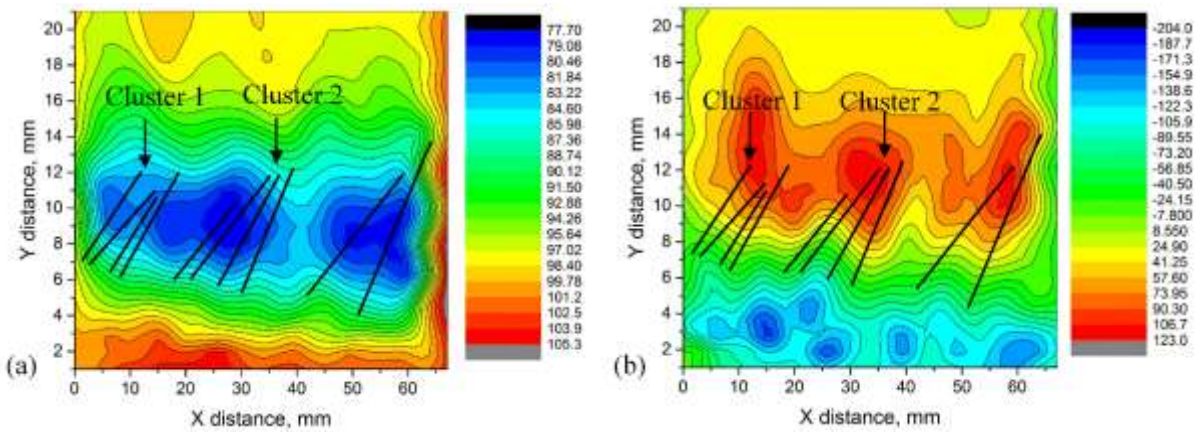

Figure 11 (a) Bx and (b) Bz signal maps using grid scanning with an ACFM pencil sensor; crack positions are superimposed on the map by black lines (not to scale). Note the two cracks on the right hand side of the sample are >20 mm in surface length (severe category) and are close to the sample edge so were not considered.

Table 5 shows the predicted dimensions (from the Bx and Bz values) compared with the actual dimensions (determined from serial sectioning) for crack clusters 1 and 2. The

$\Delta Bx_{max}/Bx_0$ values and the Bz trough-peak ratios were obtained from Figure 11. The uncompensated pocket lengths are predicted using the measured Bx and surface length values by comparison to the modelling calibration curves for uniformly sized crack clusters with vertical angle of 90°. Models are based on the average surface length and average inner spacing taken from the MPI data to obtain the elliptical ratio (determined to be 1.41 and 1.38 for cluster 1 and 2 respectively) and hence pocket length. The measured Bz trough-peak value is used to obtain the vertical angle. The uncompensated pocket length gives relatively significant differences (24.1 % for cluster 1 and 37.0 % for cluster 2) to the actual pocket length.

Compensation values of 1.9 % and 2.3 % are required for crack clusters 1 and 2 respectively for the $\Delta Bx_{max}/Bx_0$ value to account for the predicted vertical angle of 33° (cluster 1) and 28° (cluster 2). Compensation values were determined following the approach discussed in the section 'Modelled Bx responses to crack clusters' using a look up table for the effect of the different crack parameters on the ACFM signal compiled from the model outputs (shown in Figures 5-9). The compensation decreases the pocket length prediction difference for both of the inspected crack clusters, however for cluster 2, a relatively large difference is still observed (24.7 %), and this is probably due to the cluster being comprised of large cracks with an elliptical ratio of 0.87. The crack sizing algorithm and the compensation are based on modelling results for semi-ellipse cracks with an elliptical ratio from 1 to 1.75, as these values were reported in the literature, and will be less accurate if used for single cracks or crack clusters with an elliptical ratio out of this range.

Hence, using the compensation based on vertical angle improves the accuracy of the prediction for pocket length. For cluster 2 the predicted error of vertical depth has been improved from 21.4 % to 7.1 % despite the error of pocket length prediction. However, it was found that the vertical depth prediction for cluster 1 is overestimated with the same error (8.3 %) as before the compensation (where an under prediction occurred). The vertical depth is overestimated but from a railway maintenance point of view, overestimations are safer as then the crack will be completely removed from the railway rails, but will reduce the overall life of the rail. The reason the vertical depth accuracy varies is that the crack is not planar; the vertical angle where the crack is longest is less than the predicted (average) vertical angle. Figure 12 shows the 3D profiles of two cracks taken from cluster 1. Crack profiles were reconstructed by vectors using the progressive milling data and it was assumed that the crack

surface length is linear. Figure 12a shows that the crack is non-planar, i.e. the vertical angle varies along the crack length. The average vertical angle of the crack shown in Figure 11a is 29.7°. Vector 11 gives the longest pocket length of 6.5 mm with a vertical angle of 18.5°, indicating vertical depth of 2.1 mm. Vector 9 gives the largest vertical angle of 31.3° with a pocket length of 4.6 mm, indicating the largest vertical depth 2.4 mm. The position of the maximum vertical depth does not necessarily coincide with the position where the maximum pocket length is seen or follow the cracks average vertical angle. Figure 12b shows the crack profile that is more planar, i.e. vertical angles are relative uniform along the crack surface length (average vertical angle is 28.6° with the minimum and maximum of 25.6° and 31.6° respectively). For cracks with planar profiles (cracks in the light category and most cracks in the moderate category, but it is in the moderate category that the crack starts to become non-planar and asymmetric [22]), the compensation algorithm for pocket length can be used and the vertical depth prediction will be more accurate. The results reported are specific to these cracks only and differences between prediction and measured are due to the different elliptical ratio and non-planar nature of the crack profile. Further work investigating whether the pocket length compensation results in increased conservatism in vertical depth prediction should be carried out.

Table 5 Results of predicted dimensions for RCF crack clusters 1 and 2 and the comparison to the actual crack dimensions.

RCF crack cluster	1	2	Measurement error
$\Delta Bx_{max}/Bx_0$, %	19.54	22.22	0.26
Bz trough-peak ratio	-1.30	-1.38	0.14
Predicted pocket length, mm	4.1	4.6	0.1
Predicted vertical angle, °	33.0	28.0	1
Predicted vertical depth, mm	2.2	2.2	0.1
Actual pocket length (averaged), mm	5.4	7.3	0.1
Actual vertical angle (averaged), °	28.6	24.2	1
Actual maximum vertical depth, mm	2.4	2.8	0.1
Relative difference for pocket length, %	24.1	37.0	-
Relative difference for vertical angle, %	13.3	13.6	-
Relative difference for vertical depth, %	8.3	21.4	-

Surface length used for compensation, mm	11.6	12.7	0.1
Inner spacing used for compensation, mm	3.9	4.4	0.1
Compensation for pocket length, %	1.9	2.3	0.1
Predicted pocket length (compensated), mm	4.8	5.5	0.1
Relative difference for pocket length (compensated), %	11.1	24.7	-
Predicted vertical depth (compensated), mm	2.6	2.6	0.1
Relative difference for vertical depth (compensated), %	8.3	7.1	-

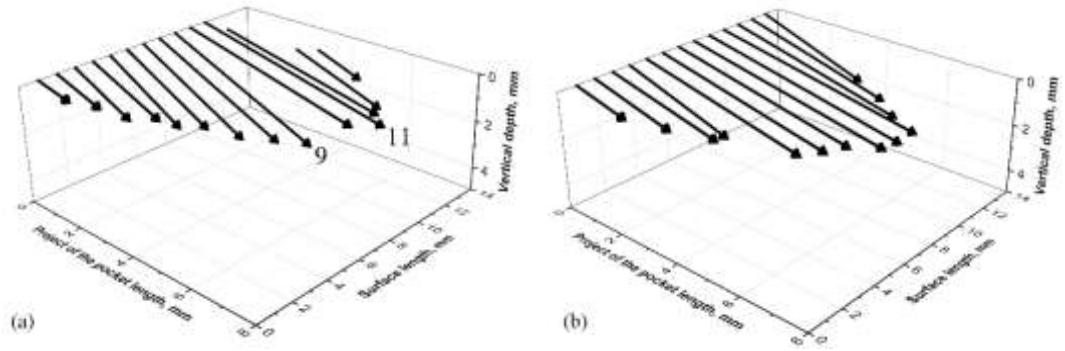

Figure 12 3D profiles of (a) non-planar and (b) approximated planer RCF cracks, where x and y axes are orthogonal axes and the x axis represents the crack surface length; the z axis is the actual vertical depth of these cracks; the arrows represent the length and position of the RCF crack determined from the progressive milling.

Conclusions

RCF cracks are complex in dimension, shape, spacing, and propagation angle into the rail, particularly for cracks present as a cluster, due to variations in train speed, axle loads and rail grades. In this paper the effects of shallow vertical angles on sizing of RCF crack clusters using an ACFM sensor have been quantitatively analysed using modelling and experimental verification. A pocket length compensation approach has been proposed to account for the effects of shallow vertical angle propagating cracks, and this approach has been applied to size real RCF crack clusters on a rail sample taken from service. Significant advances in understanding (i.e. roles of multiple crack parameters and propagation angles) and application for rail inspection are presented in this work. The main conclusions are as follows:

1. Shallow vertical angles (10-30°) have an influence on sizing of clustered RCF cracks (for different surface length, inner spacing and crack number) using ACFM signals and the influence has been quantitatively analysed using FE modelling. A pocket

length compensation method is proposed. For clustered cracks, the crack vertical angle should be predicted so that the amount of compensation for pocket length prediction can be determined according to the vertical angle range.

2. To further improve the sizing of clustered cracks in the case of shallow cracks using artificial neural network (ANN) method reported in the previous work [23]. Re-training and re-design of the ANN network on bigger datasets which also includes the ACFM response to shallow crack angles are needed.

3. Explicitly discusses the effects of crack parameters on ACFM signals for multiple RCF cracks and provides real work experimental verification. There is new understanding presented in the paper, in terms of the significance in accounting for the propagation angle into the rail, which is of generic interest to anyone trying to size non-vertical cracks.

4. Vertical angle predictions on crack clusters taken from service are close to actual values with deviations less than 13.6 %; the pocket length compensation determined by the vertical angle greatly reduced errors in the predicted pocket length from 24.1 % to 11.1 % for cluster 1 and from 37.0 % to 24.7 % for cluster 2. The predicted vertical depths using compensation agree well with the actual maximum values with errors < 8.3 % (compared to error of 60 % if sizing based on single crack). This final discrepancy is due to the non-planar crack profiles and elliptical ratio being different from models. For cracks with planar profiles (reported to be cracks in the 'light' category and most cracks in 'moderate' category, with cracks in the moderate category starting to become non-planar and asymmetric), the compensation algorithm for pocket length can be used and the vertical depth prediction will be more accurate.

Acknowledgements

The authors wish to thank the Railway Research Centre at the University of Birmingham and the Steel Processing Group from Warwick Manufacturing Group (WMG), University of Warwick, for the provision of facilities and equipment. The authors also would like to express their gratitude to TSC Inspection Systems for constructive technical discussions and Eric Magel for the provision of rail samples. The work was supported by a joint scholarship between the Chinese Scholarship Council (CSC) and the University of Warwick, UK.

References

[1] D.F. Cannon, K.O. Edel, S.L. Grassie, K. Sawley. Rail defects: an overview, Fatigue & Fracture of Engineering Materials & Structures. 2003, 26 (10): 865-886.
[2] E.E. Magel. Rolling Contact Fatigue: A Comprehensive Review, Department of Transportation-Federal railroad administration. 2011.
[3] J.E. Garnham, D.I. Fletcher, C.L. Davis, F.J. Franklin. Visualization and modelling to understand rail rolling contact fatigue cracks in three dimensions, Proceedings of the Institution of Mechanical Engineers Part F-Journal of Rail And Rapid Transit. 2011, 225 (F2): 165-178.
[4] G.L. Nicholson, H. Rowshandel, X.J. Hao, C.L. Davis. Measurement and modelling of ACFM response to multiple RCF cracks in rail and wheels, Ironmaking & Steelmaking. 2013, 40 (2): 87-91.
[5] R. Pohl, A. Erhard, H.J. Montag, H.M. Thomas, H. Wustenberg. NDT techniques for railroad wheel and gauge corner inspection, NDT & E International. 2004, 37 (2): 89-94.
[6] J.W. Ringsberg, A. Bergkvist. On propagation of short rolling contact fatigue cracks, Fatigue & Fracture of Engineering Materials & Structures. 2003, 26 (10): 969-983.
[7] J. Tillberg, F. Larsson, K. Runesson. A study of multiple crack interaction at rolling contact fatigue loading of rails, Proceedings Of the Institution Of Mechanical Engineers Part F-Journal of rail and rapid transit. 2009, 223 (4): 319-330.
[8] W. Li, G.M. Chen, C.R. Zhang, et al. Simulation analysis and experimental study of defect detection underwater by ACFM probe, China Ocean Engineering. 2013, 27 (2): 277-282.
[9] X.A. Yuan, W. Li, G.M, Chen, et al. Two-Step Interpolation Algorithm for Measurement of Longitudinal Cracks on Pipe Strings Using Circumferential Current Field Testing System. IEEE Transactions on Industrial Informatics. 2018, 14 (2): 394-402.
[10] M.P. Papaelias, C. Roberts, C.L. Davis. A review on non-destructive evaluation of rails: state-of-the-art and future development, Proceedings of the Institution of Mechanical Engineers, Part F: Journal of Rail And Rapid Transit. 2008, 222 (4): 367-384.
[11] M. Howitt. Bombardier brings ACFM into the rail industry, Insight. 2002, 44 (6): 379-382.
[12] Railtrack. Permanent way special instruction No. 4, Issue 2, 2002.
[13] H. Rowshandel. The development of an autonomous robotic inspection system to detect and characterise rolling contact fatigue cracks in railway track. PhD thesis, University of Birmingham, 2014.
[14] J. Shen, L. Zhou, H. Rowshandel, G. Nicholson, C. Davis. Determining the propagation angle for non-vertical surface-breaking cracks and its effect on crack sizing using an ACFM sensor, Measurement Science and Technology. 2015, 26 (11): 115604.
[15] D. Topp, M. Smith. Application of the ACFM inspection method to rail and rail vehicles, Insight-Non-Destructive Testing and Condition Monitoring. 2005, 47 (6): 354-357.
[16] H. Rowshandel, G.L. Nicholson, J. Shen, C.L. Davis. Characterisation of clustered rolling contact fatigue cracks in rails using an ACFM sensor and application of an artificial neural network, NDT& E International. 2018,98: 80-88.
[17] Comsol Multiphysics, 5.0 ed.

[18] G.L. Nicholson, A.G. Kostryzhev, X.J. Hao, C.L. Davis. Modelling and experimental measurements of idealised and light-moderate RCF cracks in rails using an ACFM sensor, NDT & E International. 2011, 44 (5): 427-437.
[19] G. Nicholson, C. Davis. Modelling of the response of an ACFM sensor to rail and rail wheel RCF cracks, NDT & E International. 2012, 46: 107-114.
[20] H. Rowshandel, G.L. Nicholson, C.L. Davis, C. Roberts. A robotic approach for NDT of RCF cracks in rails using an ACFM sensor, Insight. 2011, 53 (7): 368-376.
[21] H. Rowshandel, G.L. Nicholson, C.L. Davis, C. Roberts. An integrated robotic system for automatic detection and characterisation of rolling contact fatigue cracks in rails using an alternating current field measurement sensor, Proceedings of the Institution of Mechanical Engineers, Part F: Journal of Rail and Rapid Transit. 2013, 227 (4): 310-321.
[22] J. Shen. Responses of alternating current field measurement (ACFM) to rolling contact fatigue (RCF) cracks in railway rails. PhD thesis, University of Warwick, 2017.
[23] H. Rowshandel, G. Nicholson, J. Shen and C.L. Davis. An Improved Characterisation Method for Sizing Multiple Rolling Contact Fatigue Cracks in Rails using a Machine Learning Approach, NDT&E International. 2018, 98:80-88.